

Published in final edited form as:

*Biochim Biophys Acta*. 2010 September ; 1797(9): 1657–1664. doi:10.1016/j.bbabi.2010.05.010.

## Heme-heme and heme-ligand interactions in the di-heme oxygen-reducing site of cytochrome *bd* from *Escherichia coli* revealed by nanosecond absorption spectroscopy

Fabrice Rappaport<sup>a</sup>, Jie Zhang<sup>b</sup>, Marten H. Vos<sup>c,d</sup>, Robert B. Gennis<sup>b</sup>, and Vitaliy B. Borisov<sup>e,\*</sup>

<sup>a</sup>Institut de Biologie Physico-Chimique, Unite Mixte de Recherche 7141 CNRS, Universite Paris 6, 13 Rue Pierre et Marie Curie, 75005 Paris, France

<sup>b</sup>Department of Biochemistry, University of Illinois, 600 South Mathews Street, Urbana, IL 61801, USA

<sup>c</sup>Laboratoire d'Optique et Biosciences, CNRS, Ecole Polytechnique, France

<sup>d</sup>INSERM U696, F-91128 Palaiseau, France

<sup>e</sup>Belozersky Institute of Physico-Chemical Biology, Lomonosov Moscow State University, Leninskie Gory, Moscow 119991, Russian Federation

### Summary

Cytochrome *bd* is a terminal quinol:O<sub>2</sub> oxidoreductase of respiratory chains of many bacteria. It contains three hemes, *b*<sub>558</sub>, *b*<sub>595</sub>, and *d*. The role of heme *b*<sub>595</sub> remains obscure. A CO photolysis/recombination study of the membranes of *Escherichia coli* containing either wild type cytochrome *bd* or inactive E445A mutant was performed using nanosecond absorption spectroscopy. We compared photoinduced changes of heme *d*-CO complex in one-electron-reduced, two-electron-reduced, and fully-reduced states of cytochromes *bd*. The line shape of spectra of photodissociation of one-electron-reduced and two-electron-reduced enzymes is strikingly different from that of the fully-reduced enzyme. The difference demonstrates that in the fully-reduced enzyme photolysis of CO from heme *d* perturbs ferrous heme *b*<sub>595</sub> causing loss of an absorption band centered at 435 nm, thus supporting interactions between heme *b*<sub>595</sub> and heme *d* in the di-heme oxygen-reducing site, in agreement with previous works. Photolyzed CO recombines with the fully-reduced enzyme monoexponentially with  $\tau \sim 12 \mu\text{s}$ , whereas recombination of CO with one-electron-reduced cytochrome *bd* shows three kinetic phases, with  $\tau \sim 14 \text{ ns}$ ,  $14 \mu\text{s}$ , and  $280 \mu\text{s}$ . The spectra of the absorption changes associated with these components are different in line shape. The 14 ns phase, absent in the fully-reduced enzyme, reflects geminate recombination of CO with part of heme *d*. The 14  $\mu\text{s}$  component reflects bimolecular recombination of CO with heme *d* and electron backflow from heme *d* to hemes *b* in  $\sim 4\%$  of the

© 2010 Elsevier B.V. All rights reserved.

\*To whom correspondence should be addressed: Tel.: +7 495 9395149; fax: +7 495 9393181. bor@genebee.msu.su.

**Publisher's Disclaimer:** This is a PDF file of an unedited manuscript that has been accepted for publication. As a service to our customers we are providing this early version of the manuscript. The manuscript will undergo copyediting, typesetting, and review of the resulting proof before it is published in its final citable form. Please note that during the production process errors may be discovered which could affect the content, and all legal disclaimers that apply to the journal pertain.

enzyme population. The final, 280  $\mu$ s component, reflects return of the electron from hemes *b* to heme *d* and bimolecular recombination of CO in that population. The fact that even in the two-electron-reduced enzyme, a nanosecond geminate recombination is observed, suggests that namely the redox state of heme *b*<sub>595</sub>, and not that of heme *b*<sub>558</sub>, controls the pathway(s) by which CO migrates between heme *d* and the medium.

## Keywords

respiration; chlorin; cytochrome; ligand binding; gas molecule; photobiology

---

## 1. Introduction

Cytochrome *bd* is a terminal oxidase of aerobic respiratory chains of many bacteria [1–3]. It catalyzes electron transfer from quinol to molecular oxygen (to produce water) [4, 5] and couples this exergonic reaction to the generation of a membrane potential [6–10].

Apart from energy conservation, cytochrome *bd* endows bacteria with a number of specific physiological functions. Cytochrome *bd* facilitates both pathogenic and commensal bacteria to colonize oxygen-poor environments [11–14], serves as an oxygen scavenger and inhibits degradation of O<sub>2</sub>-sensitive enzymes [15], increases virulence and survival in host mammalian cells [16, 17] of pathogens, enhances bacterial tolerance to nitrosative stress [18–23], supports disulfide bond formation upon protein folding [24] and may contribute to mechanisms of detoxification of hydrogen peroxide in the bacterial cell [25].

Cytochrome *bd* is not a member of the well-known family of heme-copper oxidases. Neither of its two subunits (CydA and CydB) shows sequence homology to any subunit of heme-copper family members [26, 27]. In contrast to heme-copper oxidases, cytochrome *bd* is not a proton pump and does not contain copper in the active site [5, 28]. It contains only hemes as redox-cofactors which are heme *b*<sub>558</sub>, heme *b*<sub>595</sub> and heme *d*, with stoichiometry 1:1:1 per enzyme molecule.

The roles of the three hemes in cytochrome *bd* are different. The low-spin hexacoordinate heme *b*<sub>558</sub> is the electron entry site, it directly accepts electrons from quinol [29, 30]. The high-spin and likely pentacoordinate heme *d* is the site where binding, activation and further reduction of O<sub>2</sub> by four electrons to H<sub>2</sub>O occurs. This chlorin cofactor is likely responsible for the remarkably high affinity of the enzyme for oxygen leading to formation of a stable oxygenated complex [31, 32]. The high-spin pentacoordinate heme *b*<sub>595</sub> apparently accepts electrons from heme *b*<sub>558</sub> to deliver them to heme *d* [33, 34] but the issue as to whether this is its only role remains unanswered. A number of observations indicate that heme *b*<sub>595</sub> and heme *d* can form a common di-heme site for the oxygen reduction [8, 9, 35–43]. Nevertheless, no significant redox interactions between hemes *d* and *b*<sub>595</sub> can be observed [44]. It has also been proposed that heme *b*<sub>595</sub> may serve as a second oxygen-binding site [45, 46].

It was shown that the interaction of heme *d* with ligands differs in the fully reduced (R) enzyme (all the three hemes are reduced) and the one-electron-reduced “mixed-valence”

(MV<sup>1</sup>) enzyme (heme *d* is reduced, heme *b*<sub>558</sub> and heme *b*<sub>595</sub> are oxidized). In particular, it was found that:

- i. In the MV<sup>1</sup> CO-bound isolated WT cytochrome *bd* from *E. coli*, upon photodissociation of CO from heme *d*, a significant part of photodissociated CO (~50–70%) does not leave the protein but recombines with heme *d* within a few hundred ps. In contrast, for the enzyme in the R state under the same conditions, no such heme *d*-CO geminate recombination is observed [39, 41]. In addition, this ultrafast spectroscopy study also showed that the spectra of CO dissociation from the R and MV<sup>1</sup> forms of the WT isolated cytochrome *bd* on a picosecond time scale are different in line shape, pointing to the interaction between the close-lying hemes *d* and *b*<sub>595</sub> [39, 41]. The possible presence of later processes prior to bimolecular CO recombination has not been investigated so far.
- ii. The apparent rate constants for thermal (spontaneous) dissociation of NO and CO from the protein are much higher for the R cytochrome *bd* from *E. coli* than in case of the enzyme in the MV<sup>1</sup> state [19].
- iii. In the reaction of the R cytochrome *bd* from *Azotobacter vinelandii* with oxygen, the rate of O<sub>2</sub> binding depends linearly on the oxygen concentration up to the air level. On the contrary, when the enzyme is in the MV<sup>1</sup> state, the rate of O<sub>2</sub> binding is hyperbolic, thus revealing a saturation behavior. It was proposed that in case of the MV<sup>1</sup> cytochrome *bd*, the enzyme in equilibrium exists in the two different conformations, but only one of which can bind oxygen. When in the “closed” conformation, cytochrome *bd* provides no access for O<sub>2</sub> to heme *d*<sup>2+</sup>, whereas in the “open” conformation, oxygen binds easily. The R enzyme is always in the open conformation [32]. Thus the redox state of one or both of hemes *b* modulates ligand binding properties to heme *d*.

In the present work, we performed a systematic nanosecond study of the *E. coli* membranes containing cytochrome *bd* by varying the number of electrons in the *bd* oxidase. We used both the WT cytochrome *bd* and the E445A mutant of subunit I (CydA) that is catalytically inactive [47] and cannot be completely reduced even with excess dithionite [8]. This unique property of the mutant allowed us to generate not only the R and MV<sup>1</sup> redox states but also the two-electron-reduced (MV<sup>2</sup>) state of cytochrome *bd* which is impossible to generate in the WT and has remained uncharacterized in the previous transient absorption spectroscopy studies. Here we were able to compare in detail the photoinduced absorption changes in various redox states of the enzyme on time scales that were not investigated previously and obtain new information about the heme-heme and heme-CO interactions.

## 2. Materials and methods

### 2.1. Chemicals

Carbon monoxide was from Air Liquide; sodium dithionite was from Merck. Other basic chemicals and biochemicals were from Sigma-Aldrich, Merck, and Fluka.

## 2.2. Strains and plasmids

*E. coli* strain GO105 (*cyd AB::kan, cyo, recA*) devoid of cytochrome *bo*<sub>3</sub> and cytochrome *bd* quinol oxidases [48] was used as the host strain for expressing both the wild type and E445A mutant cytochrome *bd* from a plasmid. In both cases, plasmid pTK1 containing the whole operon encoding cytochrome *bd* and the ampicillin-resistance gene was introduced into the strain [47].

## 2.3. Cell growth and membrane preparation

The WT cells of *E. coli* were grown aerobically as reported in [39]; the E445A mutant cells were grown anaerobically as described in [47]. To obtain the *E. coli* membranes, both the WT and E445A mutant cells, washed twice with 5 mM sodium phosphate (pH 7.5), 0.17 M NaCl, and a few grains of solid 4-(2-aminoethyl)-benzenesulfonyl fluoride, were suspended in 20 mM Tris(hydroxymethyl)-aminomethan/HCl (pH 8.3), 0.5 mM ethylenediaminetetraacetate, 5 mM MgSO<sub>4</sub>, 15 mM benzamidine, 1 mM DL-dithiothreitol, 0.5 mg/L leupeptin, and a few grains of solid Deoxyribonuclease I and 4-(2-aminoethyl)-benzenesulfonyl fluoride; then the suspension was passed twice by 30-mL portions through a French press. Intact and partially broken cells were removed by centrifugation at 17,600×g for 5 min at 4 °C. The membranes were pelleted (125,000×g, 4 hrs, 4 °C), frozen in liquid nitrogen, and stored at –80 °C.

## 2.4. Sample preparation

All measurements were performed in 50 mM *N*-(2-hydroxyethyl)piperazine-*N'*-(2-ethanesulfonate)/50 mM 2-(*N*-cyclohexylamino)-ethanesulfonate (pH 8.0), and 0.5 mM ethylenediaminetetraacetate in a home-made optical cell of 2.5 mm pathway at room temperature. Cytochrome *bd* concentrations in the WT and E445A mutant membranes in the samples were 7.3 μM and 1 μM, respectively. The optical cell was first purged with argon and the sample was flowed into the cell under argon pressure. Experiments were carried out with the three stable states of carbon monoxide-bound cytochromes *bd*: (a) dithionite-reduced wild type (WT R-CO,  $b_{558}^{2+}b_{595}^{2+}d^{2+}$ -CO) and (b) dithionite-reduced mutant (E445A MV<sup>2</sup>-CO,  $b_{558}^{2+}b_{595}^{3+}d^{2+}$ -CO) were obtained by bubbling the sample, pre-reduced with 50–100 mM sodium dithionite for 30 min, with 100% CO; (c) one-electron-reduced wild type (WT MV<sup>1</sup>-CO,  $b_{558}^{3+}b_{595}^{3+}d^{2+}$ -CO) was prepared by purging the as isolated membrane-bound cytochrome *bd* (which is mainly a one-electron-reduced oxy species,  $b_{558}^{3+}b_{595}^{3+}d^{2+}$ -O<sub>2</sub>) with argon gas and then by replacing argon with 100% CO. To check the redox and ligation status of cytochrome *bd*, static absorption spectra of the samples were recorded before and after the measurements with the use of a dual pathway spectrophotometer described in [49].

## 2.5. Enzyme concentration

The cytochrome *bd* content in the *E. coli* membranes was judged from the heme *d* concentration. In the WT membranes, the heme *d* concentration was determined from the dithionite-reduced-*minus*-‘air-oxidized’ difference absorption spectra using  $\epsilon_{628-607}$  of 10.8 mM<sup>-1</sup>cm<sup>-1</sup> [38] and from the (CO-bound/dithionite-reduced)-*minus*-(dithionite-reduced) difference spectra using  $\epsilon_{643-623} = 13.2$  mM<sup>-1</sup>cm<sup>-1</sup> [10]. In the E445A mutant

membranes, the heme *d* concentration was determined from the (CO-bound/dithionite-reduced)-*minus*-(dithionite-reduced) difference spectra using  $\epsilon_{643-623} = 11.1 \text{ mM}^{-1}\text{cm}^{-1}$  that corresponds to  $\epsilon_{628-670}$  of  $25 \text{ mM}^{-1}\text{cm}^{-1}$  for the dithionite-reduced absolute absorption spectra of the isolated enzyme [8].

## 2.6. Nanosecond spectroscopy

The photoinduced absorption changes in the membranes were measured with a home-built nanosecond spectrophotometer described in [50]. The flash (excitation at 640 nm, near the  $\alpha$  band of heme *d* [44, 51, 52], 5 ns fwhm) was provided by a Nd:Yag pumped dye laser. The absorption changes were probed at discrete wavelengths and delay times after the exciting flash by flashes provided by an optical parametric oscillator pumped by the third harmonic of a Nd:Yag (5 ns fwhm).

## 2.7. Data analysis

Origin 7 (OriginLab Corporation) was used for data manipulation and presentation.

# 3. Results

## 3.1. Recombination of CO with the WT cytochrome *bd* in the R state

CO recombines with the WT cytochrome *bd* in the R state monoexponentially with  $\tau \sim 12 \mu\text{s}$  at 100% CO, as evidenced from the kinetics of flash-induced absorption changes at selected wavelengths (Fig. 1, main panel). This value corresponds to a second-order rate constant of CO recombination to heme *d* of  $\sim 8 \times 10^7 \text{ M}^{-1}\text{s}^{-1}$ , in line with the previously reported values for the isolated enzyme from *E. coli* [53] and *A. vinelandii* [40, 54]. A difference transient absorption spectrum recorded 5 ns after the flash has a reversed 'W' shape (Fig. 1, inset). Such peculiar W-shape is consistently observed as well in static Soret difference absorption spectra of CO binding to the enzyme in the R state [38, 40, 52, 55, 56].

We have previously shown that CO does not recombine with the isolated fully reduced enzyme in the time scale up to 300 ps [39]. Recent experiments (M.H.V. & V.B.B., unpublished results) have extended this range up to 4 ns. Altogether our experiments show that only bimolecular recombination occurs after dissociation of the heme *d*-CO bond in the R-CO state.

## 3.2. Recombination of CO with the WT cytochrome *bd* in the MV<sup>1</sup> state

Flash-induced absorption changes of the WT cytochrome *bd* in the MV<sup>1</sup>-CO state were monitored under the same conditions. Fig. 2A shows the transient spectra at delay times of 5 ns, 200 ns, and 60  $\mu\text{s}$ . It can be seen that the 5 ns-spectrum of the WT MV<sup>1</sup>-CO enzyme (Fig. 2A) is clearly different in line shape from its counterpart of the WT R-CO enzyme (Fig. 1, inset). The difference between the 5 ns R-CO and MV<sup>1</sup>-CO transient spectra is mainly a bleaching at 435 nm (Fig. 2D), in agreement with earlier measurements on the picoseconds time scale [41]. As shown in Fig. 2B, the spectral evolution in the WT MV<sup>1</sup> enzyme is multiphasic. It can be fitted with three exponential phases with time constants of  $\sim 14 \text{ ns}$ ,  $14 \mu\text{s}$  (10–15  $\mu\text{s}$  in different experiments), and  $280 \mu\text{s}$  (140–290  $\mu\text{s}$  in different experiments). This is in contrast to a single (12  $\mu\text{s}$ ) phase observed for the WT R enzyme

(Fig. 1). The spectra of the absorption changes associated with the three components are different in line shape. The spectrum of the 14 ns component, absent in the WT R cytochrome *bd*, reflects the decay of an induced absorption with a maximum at 435 nm (Fig. 2C), which we assign to geminate recombination of CO with part of WT MV<sup>1</sup> enzyme. The spectral characteristics of this component are similar to that of the ~100 ps phase [39] also attributed to geminate recombination. The spectrum of the absorption changes associated with the 14 μs component shows a maximum at 420 nm with a shoulder around 430 nm (Fig. 2C). This component is not homogeneous and likely reflects at least two different processes - bimolecular recombination of CO with heme *d* on the microsecond time scale and the photolysis-induced electron transfer (backflow) from heme *d* to hemes *b* in a small fraction of the enzyme molecules (see Discussion).

The spectrum of the absorption changes associated with the 280 μs component has a maximum at 438 nm and a minimum at 422 nm (Fig. 2C), and may be attributed to reversal of the electron backflow and bimolecular recombination in this enzyme fraction. According to modeling (not shown), the 280 μs component reflects re-reduction of ~3.8% of heme *d*, with the electron simultaneously returning from heme *b*<sub>595</sub> and heme *b*<sub>558</sub> in the proportion of ~70%/30%, respectively. Such relative contributions of the hemes *b* to the reversed electron transfer are consistent with those observed recently with the isolated enzyme at 1% CO [10].

### 3.3. Recombination of CO with the E445A mutant cytochrome *bd* in the MV<sup>2</sup> state

Flash-induced absorption changes of the E445A mutant cytochrome *bd* in the MV<sup>2</sup>-CO state (Fig. 3) are generally similar to those observed with the WT MV<sup>1</sup> cytochrome *bd* but also markedly different from the WT R cytochrome *bd*. Fig. 3A shows the corresponding transient spectra at 5 ns, 200 ns, and 1.5 ms. The 5 ns spectrum of the E445A MV<sup>2</sup>-CO enzyme (Fig. 3A) resembles that of the WT MV<sup>1</sup>-CO enzyme (Fig. 2A). It is worth mentioning that the 5 ns difference spectra for WT MV<sup>1</sup>-CO and E445A MV<sup>2</sup>-CO have comparable amplitudes (within a factor of 2), though the concentrations of WT and E445A differ considerably (7.3 μM vs. 1.0 μM). A few explanations of such difference which do not exclude each other can be considered. First, in MV<sup>1</sup>-CO only part of heme *d* is reduced (initially as oxy ferrous heme *d* complex), whereas in MV<sup>2</sup>-CO all heme *d* population is in the ferrous state. Therefore, after replacement of O<sub>2</sub> with CO, the actual heme *d*-CO concentration in MV<sup>1</sup>-CO should be substantially lower than 7.3 μM because neither ferryl nor oxidized heme *d* species being also present in the as-prepared MV<sup>1</sup> state can react with CO. Second, MV<sup>1</sup>-CO and MV<sup>2</sup>-CO may differ in a fraction that undergoes geminate recombination of CO and heme *d* at earlier (subnanosecond) times. If in the former case the enzyme population involved in subnanosecond recombination is larger, the amplitude at a delay time of 5 ns will become smaller. Third, the quantum yield of photodissociation of CO from heme *d* in E445A MV<sup>2</sup>-CO may be larger than that in WT MV<sup>1</sup>-CO.

The kinetics of CO recombination at selected wavelengths for the MV<sup>2</sup>-CO state (Fig. 3B, symbols) can be reasonably fitted with two exponentials (Fig. 3B, solid lines) with time constants of ~14 ns, and 42 μs (38–42 μs in different experiments). Using three exponentials does not improve fit significantly. These changes can mainly reflect geminate and



bimolecular recombination of CO with heme *d* on the nanosecond and microsecond time scales, respectively. Remarkably, the 280  $\mu$ s component observed in the MV<sup>1</sup> state is absent. This implies that under these conditions back electron transfer from heme *d* to heme *b*<sub>595</sub> requires heme *b*<sub>558</sub> to be in the oxidized state.

The spectrum of the bimolecular recombination component differs somewhat from the nanosecond component. This may be due to interaction of dissociated CO with the hemes while it is sequestered close to the active site.

CO recombination to the E445A MV<sup>2</sup> enzyme (Fig.3B) appeared to be about 3-fold slower than that to the WT MV<sup>1</sup> cytochrome *bd* (Fig. 2B). Two possible explanations can be suggested. First, the mutation could affect an access channel for ligand transfer between the bulk phase and heme *d*. The existence of such channel(s) in cytochrome *bd* has been proposed earlier [19, 32, 39]. Second, the mutation could decrease the affinity of ferrous heme *d* for CO.

#### 4. Discussion

Earlier, recombination of CO with the dithionite-reduced *E. coli* membranes containing the WT cytochrome *bd* was studied on the micro/millisecond time scale at the 532 nm excitation [57]. These membranes were treated with detergent. Treatment of membrane-bound cytochrome *bd* with detergent can markedly attenuate scattering in the near UV typical of the native membranes that allowed resolving flash-induced absorption changes in the Soret. However, treatment of cytochrome *bd* with detergent can lead to appearance of a denatured fraction of heme *b* reacting with CO [2, 56]. Such a heme *b*-CO complex can be easily photolyzed at the 532 nm excitation that resulted in additional slower phases of CO recombination with heme *b* [40, 54, 57], significantly complicating interpretation of the data [57]. In the present experiments, native membranes of *E. coli*, devoid of such an undesired reaction, were used. The use of a specific set-up in the photolysis experiments allows us to monitor absorption changes with a very high resolution even in the near UV region, starting from the time of 5 ns (see the Materials and methods section). Upon selective excitation of the  $\alpha$  band of heme *d* (at 640 nm), CO is photolyzed only from heme *d*.

In the present study we showed that at the 640 nm excitation the flash-induced absorption changes for the *E. coli* membranes containing the WT cytochrome *bd* in the R-CO and MV<sup>1</sup>-CO states under the same conditions differ in (i) line shape of the transient spectra, (ii) number of recombination phases, (iii) amplitude of the response.

(i) As previously observed for the picosecond CO photodissociation spectra of the isolated WT enzyme [41], the transient spectra at 5 ns of the WT membranes containing cytochrome *bd* in the R and MV<sup>1</sup> states are clearly different in line shape. The WT R spectrum has a reversed W-shape with a *minimum* at 435 nm (Fig. 1, inset) whereas the main feature of that of the WT MV<sup>1</sup> is the *maximum* at 435 nm (Fig. 2A). The difference between the normalized R and MV<sup>1</sup> spectra is the bleaching at 435 nm (Fig. 2D) [41]. An explanation suggested in [39, 41] for the picosecond spectra is that in the R enzyme photolysis of CO from heme *d* perturbs ferrous heme *b*<sub>595</sub> causing loss of an absorption band centered at 435

nm. The data of nanosecond spectroscopy support this conclusion and further substantiate the assignment of the bleaching at 435 nm (Fig. 2D) to the interaction between heme *d* and heme *b*<sub>595</sub>.

(ii) One of the main results of this work is that the dynamics of the flash-induced absorption changes for WT cytochrome *bd* is strikingly different in the R-CO and MV<sup>1</sup>-CO states. In R-CO, there is a single phase of bimolecular recombination with  $\tau \sim 12 \mu\text{s}$  at 1 atm CO (Fig. 1). In contrast, in MV<sup>1</sup>-CO, there are three phases of recombination with time constants of  $\sim 14 \text{ ns}$ ,  $14 \mu\text{s}$ , and  $280 \mu\text{s}$  (Fig. 2B) plus a picosecond phase of geminate recombination ( $\tau \sim 70\text{--}200 \text{ ps}$ ) observed earlier [39]. Thus, there are totally four phases in MV<sup>1</sup>-CO.

The line shape of the spectra associated with the three phases of recombination in MV<sup>1</sup>-CO is different. The spectrum of the 14 ns component, absent in the R enzyme, is the induced absorption with a maximum at 435 nm (Fig. 2C), very similar to the ps MV<sup>1</sup>-CO spectrum [41]. This similarity allows us to suggest that the 14 ns component reflects a second phase of geminate recombination of CO with heme *d* in part of MV<sup>1</sup>, following the  $\sim 100 \text{ ps}$  phase [39]. The presence of at least two phases of CO geminate recombination indicates the presence of several distinct configurations of non-bound CO within the protein moiety. As discussed previously [39], the absence of geminate recombination in the fully reduced enzyme implies that the redox state of heme *b*<sub>595</sub> controls the pathways of unbound CO. Our present finding of a second geminate rebinding phase also only in MV complexes indicates that all geminate rebinding to heme *d* is influenced by heme *b*<sub>595</sub>, suggesting that the nanosecond rebinding occurs via the conformation from which picosecond rebinding occurs (Fig. 4A), in agreement with the proposed proximity of hemes *d* and *b*<sub>595</sub>.

Based on transmembrane electron transfer kinetics observed in previous electrogenicity studies (Fig. 7, trace 3 in Ref. [7]), and of our modeling of the 280  $\mu\text{s}$  phase, we propose that the 14  $\mu\text{s}$  and 280  $\mu\text{s}$  heme *d* – CO recombination phases also reflect backflow (14  $\mu\text{s}$  phase) and reverse backflow (280  $\mu\text{s}$  phase) between heme *d* and the *b* hemes. Fig. 4B depicts a scheme encompassing the ensemble of competing reactions on the microsecond time scale that summarizes our interpretation of the data, as discussed below.

In this view, the 14  $\mu\text{s}$  component consists of at least two different processes: (a) bimolecular recombination of CO with the remaining ferrous unligated heme *d* on the microsecond time scale, and (b) the electron backflow from heme *d* to hemes *b* in  $\sim 3.8\%$  of the enzyme molecules (see Fig. 4B).

The conclusion that the 14  $\mu\text{s}$  component includes recombination of CO with heme *d* that is bimolecular rather than geminate is based on the data of Junemann et al. [58] who first observed such recombination with the *A. vinelandii* cytochrome *bd* in the MV<sup>1</sup> state monitoring the heme *d*  $\alpha$ -band. They showed that the rate of recombination increases linearly with the CO concentration, hence the recombination is indeed bimolecular. Their observation that the second-order rate constant of recombination for the MV<sup>1</sup> enzyme ( $1 \times 10^8 \text{ M}^{-1}\text{s}^{-1}$ ) is only slightly slower than that for the R enzyme ( $1.5 \times 10^8 \text{ M}^{-1}\text{s}^{-1}$ ) [58] is also in agreement with our data.



Another factor that contributes to this phase is electron redistribution from heme *d* to hemes *b* in ~ 3.8% of the MV<sup>1</sup> cytochrome *bd* induced by photolysis. This is in agreement with the spectrum of the next, 280 μs component, showing a maximum at 438 nm and a minimum at 422 nm (Fig. 2C), that reflects return of the electron from the hemes *b* to heme *d*. It is worth to mention that, even under optimum conditions, the amplitude of the electron backflow is quite small due to the large redox potential difference between *d* and *b* hemes. Furthermore, since there is a competition between CO recombination and backflow [7], the backflow could previously be detected by micro/millisecond absorption spectroscopy only at low CO concentrations [7, 58]. At 1% CO, ~ 11% of heme *d* is oxidized following CO photolysis and the electron simultaneously moves to hemes *b*<sub>558</sub> and *b*<sub>595</sub> [10] and then returns back as CO recombines. At 100% CO, no internal electron redistribution in the MV<sup>1</sup> cytochrome *bd* has been detected by absorption spectroscopy hitherto. The reverse electron flow was found to be associated with the generation of membrane potential [7]. The finding that the signal-to-noise ratio of electrometric traces is superior to that of absorbance traces allowed us to observe electrometric backflow transients even at high CO concentrations [7]. At 100% CO, the electron backflow is present but its amplitude decreases to be of about one-fourth of that at 1% CO (see Fig. 7 of [7]), i.e. around 3% of heme *d* can be oxidized following CO photolysis provided this value is 11% at 1% CO. The electrometric backflow response decays with time constant of about 360 μs [7] that is in rough agreement with the 280 μs phase observed in this work. Owing to the fact that extinction of hemes *b* in the Soret is much larger than that of heme *d* [44] and due to a very high sensitivity of the technique used, we are now able to observe spectrophotometrically flash-induced internal electron redistribution and its relaxation even at 100% CO.

It should be noted that the 280 μs component is not observed in the MV<sup>2</sup>-CO enzyme (Fig. 3). This agrees with our conclusion about the origin of the microsecond phases in the MV<sup>1</sup>-CO cytochrome *bd* because flash-induced electron redistribution between hemes *d* and *b*<sub>558</sub> is not possible in the MV<sup>2</sup>-CO state (both hemes are reduced in this state). Electron backflow from heme *d* to heme *b*<sub>595</sub> in the E445A MV<sup>2</sup>-CO enzyme is apparently also negligible under these conditions. As such electron transfer does occur to a significant extent starting from the MV<sup>1</sup>-CO state, this finding implies that the redox state of heme *b*<sub>558</sub> influences the redox potential difference between hemes *d* and *b*<sub>595</sub>. This reasoning is consistent with the report of negative redox interactions between hemes *b*<sub>558</sub> and *b*<sub>595</sub> [44]. The fact that the difference between the normalized spectra of the 14 μs phase for MV<sup>1</sup>-CO and the 42 μs phase for MV<sup>2</sup>-CO (not shown) is similar to the reversed spectrum of the 280 μs component further supports such conclusion.

It has to be noted that the lack of heme *b*<sub>595</sub> reduction in photolyzed MV<sup>2</sup>-CO state seems to contrast with a report of Belevich et al. [8] where such reduction was observed. The experimental conditions of that work were different: it was carried out with the isolated detergent-solubilized enzyme, at 1% CO, the kinetics of the electron transfer was not resolved [8]. Two possible explanations of such apparent discrepancy can be suggested. First, due to the mutation, the rate of electron transfer between the hemes may become slower in the E445A enzyme as compared to the WT enzyme. Since, as mentioned above, there must be a competition between CO recombination and backflow, at 100% CO used in

this study, the photolysis-induced electron transfer from heme *d* to heme *b*<sub>595</sub> may be indeed negligible by that reason. Second, the midpoint potential values for WT cytochrome *bd* from *E. coli* can significantly depend on the nature of membrane environment such as detergent used for the enzyme solubilization [59]. The latter has never been tested with the E445A mutant cytochrome *bd*. It is possible that in the mutant cytochrome *bd* of the bacterial membranes (this work)  $E_m$  between heme *d* and heme *b*<sub>595</sub> is larger (i.e.,  $E_m$  of *b*<sub>595</sub> is lower) than that in the isolated detergent-solubilized enzyme [8] that in the former case would make the electron backflow thermodynamically unfavorable to occur. The combination of these two reasons cannot also be excluded.

(iii) R-CO and MV<sup>1</sup>-CO WT cytochromes *bd* differ in the yield of the observed photolysis of CO from ferrous heme *d* at 5 ns. Although recorded under the same enzyme concentration and other experimental conditions, a normalization factor of ~7.5 is required for the 5 ns WT MV<sup>1</sup>-CO transient spectrum to match that of R-CO, provided the extinction coefficients of R-CO and MV<sup>1</sup>-CO at 445 nm are virtually identical [41]. Since in the “as prepared” state of WT cytochrome *bd* used to generate MV<sup>1</sup>-CO, only about 70% of heme *d* is in the oxy form (MV<sup>1</sup>-O<sub>2</sub>), the actual factor is ~5.2. This means that in case of WT MV<sup>1</sup> cytochrome *bd*, no more than ~20% of ferrous heme *d* can be observed as recombining with CO through a bimolecular mechanism on the microsecond time scale. This is in full agreement with the picosecond studies where in at least half of the photolyzed WT MV<sup>1</sup>-CO purified enzyme, subnanosecond geminate recombination of CO and heme *d* occurs [39] and the quantum yield of photodissociation of CO from heme *d* was found to be ~3-fold diminished in the presence of oxidized hemes *b* [41].

In all earlier studies where ligand-reaction pattern was compared for WT cytochrome *bd* in R and MV<sup>1</sup> states and the differences were observed [19, 32, 39, 41], the redox state of which of the two *b* hemes modulates ligand binding/dissociation properties of the heme *d* active site, was not established. This could be heme *b*<sub>595</sub>, or heme *b*<sub>558</sub>, or both. In this work we used the E445A mutant cytochrome *bd* in which heme *b*<sub>595</sub> remains in the ferric state even in the presence of a strong reductant. This unique possibility to have two-electron-reduced mixed-valence enzyme (MV<sup>2</sup>) was used to answer this question. First, we found that the line shape of the photodissociation spectrum (at a delay time of 5 ns) of the E445A mutant in the MV<sup>2</sup>-CO state (Fig. 3A) is similar to that of the WT cytochrome *bd* in the MV<sup>1</sup>-CO state (Fig. 2A) but strikingly different from that of the WT enzyme in the R state (Fig. 1, inset). In contrast to the latter spectrum, it does not display the sharp bleaching feature at 435 nm as clearly demonstrates the difference between the 5 ns transient spectra of the WT R and E445A MV<sup>2</sup> cytochromes *bd* (Fig. 3C). This difference is also reminiscent of that between the picosecond transient spectra of the R and MV<sup>1</sup> purified enzymes under isotropic conditions [41]. Hence we can conclude that dissociation of CO from heme *d* perturbs the Soret band of heme *b*<sub>595</sub> but not that of heme *b*<sub>558</sub>. The data thus further support interactions between high-spin protoporphyrin *b*<sub>595</sub> and chlorin *d* in the di-heme oxygen-reducing site, in agreement with previous works [8, 9, 36–43].

Second, in the case of E445A MV<sup>2</sup>-CO, apart from a microsecond phase of bimolecular recombination, there is also an additional phase of CO recombination on the nanosecond time scale with  $\tau \sim 14$  ns (Fig. 3), absent in the WT R cytochrome *bd*. The fact that the

spectrum of the 14 ns component of E445A MV<sup>2</sup>-CO is very similar in line shape to that of WT MV<sup>1</sup>-CO (Fig. 3D), supports the conclusion that also in E445A MV<sup>2</sup>-CO cytochrome *bd* geminate recombination of CO with heme *d* on the nanosecond time scale occurs. Thus, the redox state of heme *b*<sub>595</sub> controls the pathway(s) by which CO migrates between heme *d* and the medium. In light of this finding we can also suggest that the same holds true for O<sub>2</sub> [32] and NO [19].

## Acknowledgments

This work was supported by the Russian Foundation for Basic Research (to V.B.B., grant 08-04-00093). V.B.B. was recipient of a FEBS short-term fellowship. We thank Dr. Pierre Joliot (Paris) and Dr. Alexander Konstantinov (Moscow) for their interest and stimulating discussions of this work.

## Abbreviations

<b>WT</b>	wild type
<b>R</b>	fully reduced (three-electron-reduced) species ( $b_{558}^{2+}b_{595}^{2+}d^{2+}$ )
<b>MV<sup>1</sup></b>	one-electron-reduced “mixed-valence” species ( $b_{558}^{3+}b_{595}^{3+}d^{2+}$ )
<b>MV<sup>2</sup></b>	two-electron-reduced “mixed-valence” species ( $b_{558}^{2+}b_{595}^{3+}d^{2+}$ )
<b>fwhm</b>	full width at half-maximum
<b><math>\tau</math></b>	time constant, reciprocal of rate constant, $t_{1/e}$

## References

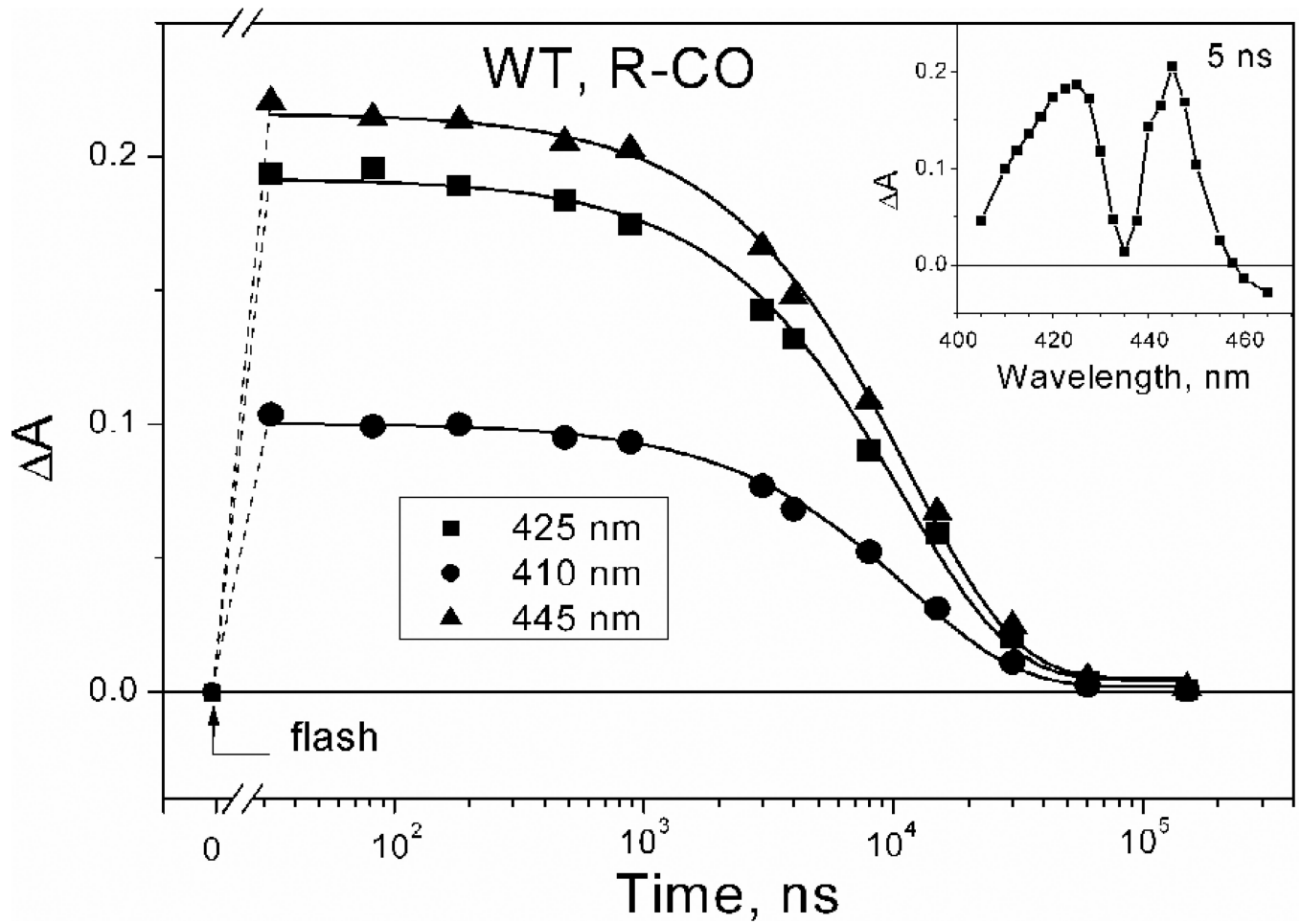
1. Poole RK, Cook GM. Redundancy of aerobic respiratory chains in bacteria? Routes, reasons and regulation. *Adv. Microb. Physiol.* 2000; 43:165–224. [PubMed: 10907557]
2. Junemann S. Cytochrome *bd* terminal oxidase. *Biochim. Biophys. Acta.* 1997; 1321:107–127. [PubMed: 9332500]
3. Borisov VB. Cytochrome *bd*: structure and properties. *Biochemistry (Moscow)*. 1996; 61:565–574. (translated from *Biokhimiya* (in Russian) (1996), 61, 786–799).
4. Tsubaki M, Hori H, Mogi T. Probing molecular structure of dioxygen reduction site of bacterial quinol oxidases through ligand binding to the redox metal centers. *J. Inorg. Biochem.* 2000; 82:19–25. [PubMed: 11132627]
5. Borisov, VB.; Verkhovsky, MI. Oxygen as acceptor [Chapter 3.2.7]. In: Böck, A.; Curtiss, R., III; Kaper, JB.; Neidhardt, FC.; Nyström, T.; Rudd, KE.; Squires, CL., editors. *EcoSal - Escherichia coli and Salmonella: cellular and molecular biology*. Washington, DC: ASM Press; 2009. <<http://www.ecosal.org>>
6. Puustinen A, Finel M, Haltia T, Gennis RB, Wikstrom M. Properties of the two terminal oxidases of *Escherichia coli*. *Biochemistry*. 1991; 30:3936–3942. [PubMed: 1850294]
7. Jasaitis A, Borisov VB, Belevich NP, Morgan JE, Konstantinov AA, Verkhovsky MI. Electrogenic reactions of cytochrome *bd*. *Biochemistry*. 2000; 39:13800–13809. [PubMed: 11076519]
8. Belevich I, Borisov VB, Zhang J, Yang K, Konstantinov AA, Gennis RB, Verkhovsky MI. Time-resolved electrometric and optical studies on cytochrome *bd* suggest a mechanism of electron-proton coupling in the di-heme active site. *Proc. Natl. Acad. Sci. USA.* 2005; 102:3657–3662. [PubMed: 15728392]
9. Belevich I, Borisov VB, Verkhovsky MI. Discovery of the true peroxy intermediate in the catalytic cycle of terminal oxidases by real-time measurement. *J. Biol. Chem.* 2007; 282:28514–28519. [PubMed: 17690093]

10. Borisov VB, Belevich I, Bloch DA, Mogi T, Verkhovsky MI. Glutamate 107 in subunit I of cytochrome *bd* from *Escherichia coli* is part of a transmembrane intraprotein pathway conducting protons from the cytoplasm to the heme *b<sub>595</sub>*/heme *d* active site. *Biochemistry*. 2008; 47:7907–7914. [PubMed: 18597483]
11. Baughn AD, Malamy MH. The strict anaerobe *Bacteroides fragilis* grows in and benefits from nanomolar concentrations of oxygen. *Nature*. 2004; 427:441–444. [PubMed: 14749831]
12. Shi L, Sohaskey CD, Kana BD, Dawes S, North RJ, Mizrahi V, Gennaro ML. Changes in energy metabolism of *Mycobacterium tuberculosis* in mouse lung and under in vitro conditions affecting aerobic respiration. *Proc. Natl. Acad. Sci. USA*. 2005; 102:15629–15634. [PubMed: 16227431]
13. Loisel-Meyer S, Jimenez de Bagues MP, Kohler S, Liautard JP, Jubier-Maurin V. Differential use of the two high-oxygen-affinity terminal oxidases of *Brucella suis* for in vitro and intramacrophagic multiplication. *Infect. Immun*. 2005; 73:7768–7771. [PubMed: 16239582]
14. Jones SA, Chowdhury FZ, Fabich AJ, Anderson A, Schreiner DM, House AL, Autieri SM, Leatham MP, Lins JJ, Jorgensen M, Cohen PS, Conway T. Respiration of *Escherichia coli* in the mouse intestine. *Infect. Immun*. 2007; 75:4891–4899. [PubMed: 17698572]
15. Hill S, Viollet S, Smith AT, Anthony C. Roles for enteric *d*-type cytochrome oxidase in N<sub>2</sub> fixation and microaerobiosis. *J. Bacteriol*. 1990; 172:2071–2078. [PubMed: 2156809]
16. Way SS, Sallustio S, Magliozzo RS, Goldberg MB. Impact of either elevated or decreased levels of cytochrome *bd* expression on *Shigella flexneri* virulence. *J. Bacteriol*. 1999; 181:1229–1237. [PubMed: 9973350]
17. Endley S, McMurray D, Ficht TA. Interruption of the *cydB* locus in *Brucella abortus* attenuates intracellular survival and virulence in the mouse model of infection. *J. Bacteriol*. 2001; 183:2454–2462. [PubMed: 11274104]
18. Borisov VB, Forte E, Konstantinov AA, Poole RK, Sarti P, Giuffre A. Interaction of the bacterial terminal oxidase cytochrome *bd* with nitric oxide. *FEBS Lett*. 2004; 576:201–204. [PubMed: 15474037]
19. Borisov VB, Forte E, Sarti P, Brunori M, Konstantinov AA, Giuffre A. Redox control of fast ligand dissociation from *Escherichia coli* cytochrome *bd*. *Biochem. Biophys. Res. Commun*. 2007; 355:97–102. [PubMed: 17280642]
20. Mason MG, Shepherd M, Nicholls P, Dobbin PS, Dodsworth KS, Poole RK, Cooper CE. Cytochrome *bd* confers nitric oxide resistance to *Escherichia coli*. *Nat. Chem. Biol*. 2009; 5:94–96. [PubMed: 19109594]
21. Forte E, Borisov VB, Konstantinov AA, Brunori M, Giuffre A, Sarti P. Cytochrome *bd* a key oxidase in bacterial survival and tolerance to nitrosative stress. *Ital. J. Biochem*. 2007; 56:265–269. [PubMed: 19192624]
22. Borisov VB, Forte E, Sarti P, Brunori M, Konstantinov AA, Giuffre A. Nitric oxide reacts with the ferryl-oxo catalytic intermediate of the Cu<sub>B</sub>-lacking cytochrome *bd* terminal oxidase. *FEBS Lett*. 2006; 580:4823–4826. [PubMed: 16904110]
23. Borisov VB, Forte E, Giuffre A, Konstantinov A, Sarti P. Reaction of nitric oxide with the oxidized di-heme and heme-copper oxygen-reducing centers of terminal oxidases: Different reaction pathways and end-products. *J. Inorg. Biochem*. 2009; 103:1185–1187. [PubMed: 19592112]
24. Bader M, Muse W, Ballou DP, Gassner C, Bardwell JCA. Oxidative protein folding is driven by the electron transport system. *Cell*. 1999; 98:217–227. [PubMed: 10428033]
25. Borisov VB, Davletshin AI, Konstantinov AA. Peroxidase activity of cytochrome *bd* from *Escherichia coli*. *Biochemistry (Moscow)*. 2010; 75:428–436. (translated from *Biokhimiya* (in Russian) (2010), 75, 520–530). [PubMed: 20618131]
26. Green GN, Fang H, Lin R-J, Newton G, Mather M, Georgiou CD, Gennis RB. The nucleotide sequence of the *cyd* locus encoding the two subunits of the cytochrome *d* terminal oxidase complex of *Escherichia coli*. *J. Biol. Chem*. 1988; 263:13138–13143. [PubMed: 2843510]
27. Poole RK. Oxygen reactions with bacterial oxidases and globins: binding, reduction and regulation. *Antonie van Leeuwenhoek*. 1994; 65:289–310.

28. Mogi T, Tsubaki M, Hori H, Miyoshi H, Nakamura H, Anraku Y. Two terminal quinol oxidase families in *Escherichia coli*: variations on molecular machinery for dioxygen reduction. *J. Biochem. Mol. Biol. Biophys.* 1998; 2:79–110.
29. Junemann S, Wrigglesworth JM. Antimycin inhibition of the cytochrome *bd* complex from *Azotobacter vinelandii* indicates the presence of a branched electron transfer pathway for the oxidation of ubiquinol. *FEBS Lett.* 1994; 345:198–202. [PubMed: 8200455]
30. Spinner F, Cheesman MR, Thomson AJ, Kaysser T, Gennis RB, Peng Q, Peterson J. The haem *b*<sub>558</sub> component of the cytochrome *bd* quinol oxidase complex from *Escherichia coli* has histidine-methionine axial ligation. *Biochem. J.* 1995; 308:641–644. [PubMed: 7772053]
31. Belevich I, Borisov VB, Konstantinov AA, Verkhovskiy MI. Oxygenated complex of cytochrome *bd* from *Escherichia coli*: stability and photolability. *FEBS Lett.* 2005; 579:4567–4570. [PubMed: 16087180]
32. Belevich I, Borisov VB, Bloch DA, Konstantinov AA, Verkhovskiy MI. Cytochrome *bd* from *Azotobacter vinelandii*: evidence for high-affinity oxygen binding. *Biochemistry.* 2007; 46:11177–11184. [PubMed: 17784736]
33. Poole RK, Williams HD. Proposal that the function of the membrane-bound cytochrome *a*<sub>1</sub>-like haemoprotein (cytochrome *b*-595) in *Escherichia coli* is a direct electron donation to cytochrome *d*. *FEBS Lett.* 1987; 217:49–52. [PubMed: 3036575]
34. Kobayashi K, Tagawa S, Mogi T. Electron transfer process in cytochrome *bd*-type ubiquinol oxidase from *Escherichia coli* revealed by pulse radiolysis. *Biochemistry.* 1999; 38:5913–5917. [PubMed: 10231544]
35. Krasnoselskaya I, Arutjunjan AM, Smirnova I, Gennis R, Konstantinov AA. Cyanidoreactive sites in cytochrome *bd* complex from *E. coli*. *FEBS Lett.* 1993; 327:279–283. [PubMed: 8348954]
36. Hill JJ, Alben JO, Gennis RB. Spectroscopic evidence for a heme-heme binuclear center in the cytochrome *bd* ubiquinol oxidase from *Escherichia coli*. *Proc. Natl. Acad. Sci. USA.* 1993; 90:5863–5867. [PubMed: 8516338]
37. Tsubaki M, Hori H, Mogi T, Anraku Y. Cyanide-binding site of *bd*-type ubiquinol oxidase from *Escherichia coli*. *J. Biol. Chem.* 1995; 270:28565–28569. [PubMed: 7499371]
38. Borisov V, Arutyunyan AM, Osborne JP, Gennis RB, Konstantinov AA. Magnetic circular dichroism used to examine the interaction of *Escherichia coli* cytochrome *bd* with ligands. *Biochemistry.* 1999; 38:740–750. [PubMed: 9888814]
39. Vos MH, Borisov VB, Liebl U, Martin J-L, Konstantinov AA. Femtosecond resolution of ligand-heme interactions in the high-affinity quinol oxidase *bd*: A di-heme active site? *Proc. Natl. Acad. Sci. USA.* 2000; 97:1554–1559. [PubMed: 10660685]
40. Borisov VB, Sedelnikova SE, Poole RK, Konstantinov AA. Interaction of cytochrome *bd* with carbon monoxide at low and room temperatures: evidence that only a small fraction of heme *b*<sub>595</sub> reacts with CO. *J. Biol. Chem.* 2001; 276:22095–22099. [PubMed: 11283005]
41. Borisov VB, Liebl U, Rappaport F, Martin J-L, Zhang J, Gennis R.B, Konstantinov AA, Vos MH. Interactions between heme *d* and heme *b*<sub>595</sub> in quinol oxidase *bd* from *Escherichia coli*: a photoselection study using femtosecond spectroscopy. *Biochemistry.* 2002; 41:1654–1662. [PubMed: 11814360]
42. Hori H, Tsubaki M, Mogi T, Anraku Y. EPR study of NO complex of *bd*-type ubiquinol oxidase from *Escherichia coli*. *J. Biol. Chem.* 1996; 271:9254–9258. [PubMed: 8621585]
43. Arutyunyan AM, Borisov VB, Novoderezhkin VI, Ghaim J, Zhang J, Gennis RB, Konstantinov AA. Strong excitonic interactions in the oxygen-reducing site of *bd*-type oxidase: the Fe-to-Fe distance between hemes *d* and *b*<sub>595</sub> is 10 Å. *Biochemistry.* 2008; 47:1752–1759. [PubMed: 18205406]
44. Bloch DA, Borisov VB, Mogi T, Verkhovskiy MI. Heme/heme redox interaction and resolution of individual optical absorption spectra of the hemes in cytochrome *bd* from *Escherichia coli*. *Biochim. Biophys. Acta.* 2009; 1787:1246–1253. [PubMed: 19450539]
45. Rothery RA, Houston AM, Ingledew WJ. The respiratory chain of anaerobically grown *Escherichia coli*: Reactions with nitrite and oxygen. *J. Gen. Microbiol.* 1987; 133:3247–3255. [PubMed: 2833564]

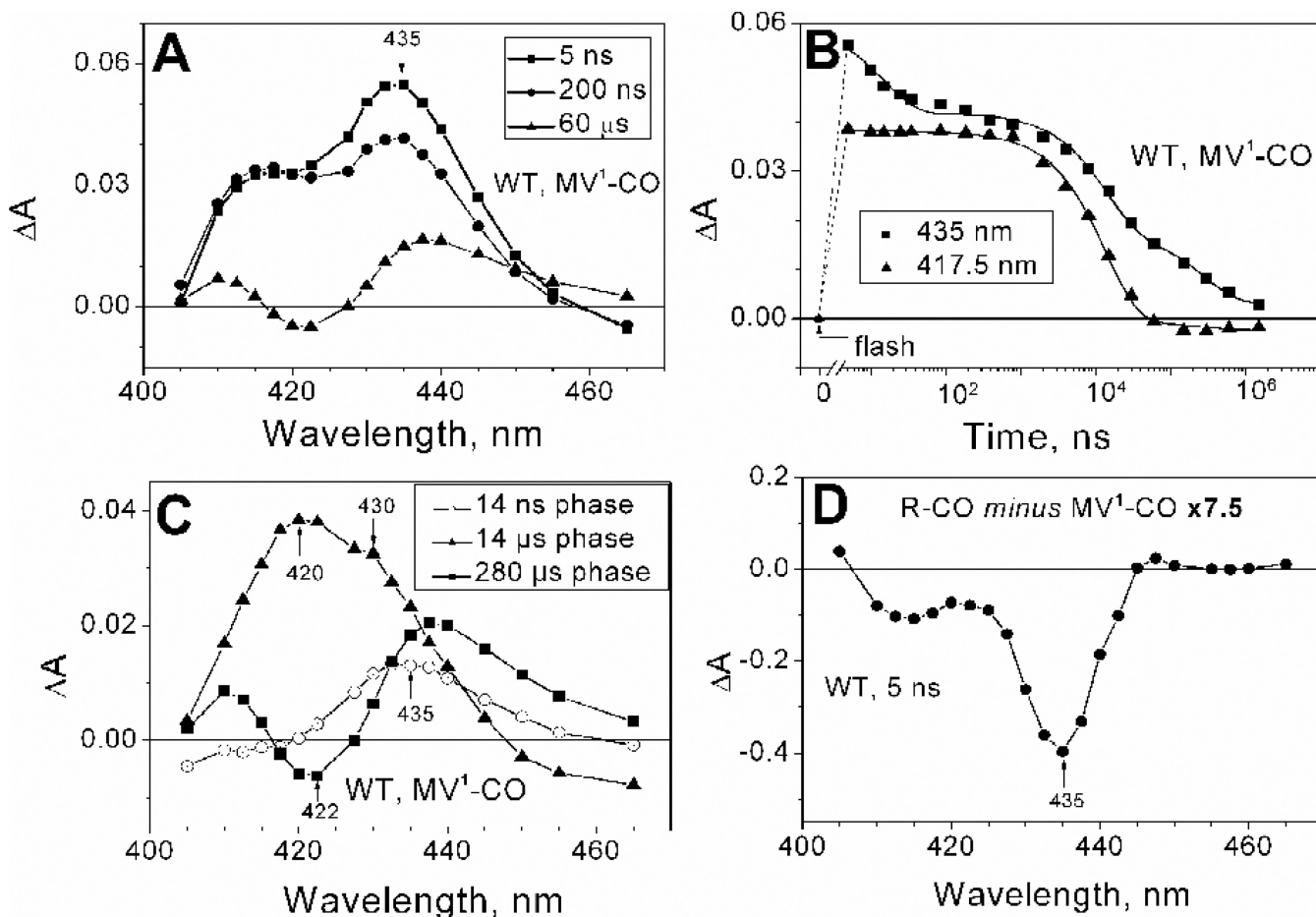
46. D'mello R, Hill S, Poole RK. The Cytochrome *bd* quinol oxidase in *Escherichia coli* has an extremely high oxygen affinity and two-oxygen-binding haems: implications for regulation of activity *in vivo* by oxygen inhibition. *Microbiology*. 1996; 142:755–763. [PubMed: 8936304]
47. Zhang J, Hellwig P, Osborne JP, Huang HW, Moenne-Loccoz P, Konstantinov AA, Gennis RB. Site-directed mutation of the highly conserved region near the Q-loop of the cytochrome *bd* quinol oxidase from *Escherichia coli* specifically perturbs heme *b<sub>595</sub>*. *Biochemistry*. 2001; 40:8548–8556. [PubMed: 11456494]
48. Kaysser TM, Ghaim JB, Georgiou C, Gennis RB. Methionine-393 is an axial ligand of the heme *b<sub>558</sub>* component of the cytochrome *bd* ubiquinol oxidase from *Escherichia coli*. *Biochemistry*. 1995; 34:13491–13501. [PubMed: 7577938]
49. Joliot P, Beal D, Frilley B. Une nouvelle methode spectrophotometrique destinee a l'etude des reactions photosynthetiques. *Journal de chimie physique*. 1980; 77:209–216.
50. Beal D, Rappaport F, Joliot P. A new high-sensitivity 10-ns time-resolution spectrophotometric technique adapted to *in vivo* analysis of the photosynthetic apparatus. *Rev. Sci. Instrum.* 1999; 70:202–207.
51. Koland JG, Miller MJ, Gennis RB. Potentiometric analysis of the purified cytochrome *d* terminal oxidase complex from *Escherichia coli*. *Biochemistry*. 1984; 23:1051–1056.
52. Lorence RM, Koland JG, Gennis RB. Coulometric and spectroscopic analysis of the purified cytochrome *d* complex of *Escherichia coli*: Evidence for the identification of "cytochrome *a<sub>1</sub>*" as cytochrome *b<sub>595</sub>*. *Biochemistry*. 1986; 25:2314–2321. [PubMed: 3013299]
53. Hill BC, Hill JJ, Gennis RB. The room temperature reaction of carbon monoxide and oxygen with the cytochrome *bd* quinol oxidase from *Escherichia coli*. *Biochemistry*. 1994; 33:15110–15115. [PubMed: 7999770]
54. Junemann S, Rich PR, Wrigglesworth JM. CO flash photolysis of cytochrome *bd* from *Azotobacter vinelandii*. *Biochem. Soc. Trans.* 1995; 23:157S. [PubMed: 7672188]
55. Junemann S, Wrigglesworth JM. Cytochrome *bd* oxidase from *Azotobacter vinelandii*. Purification and quantitation of ligand binding to the oxygen reduction site. *J. Biol. Chem.* 1995; 270:16213–16220. [PubMed: 7608187]
56. Borisov VB. Interaction of *bd*-type quinol oxidase from *Escherichia coli* and carbon monoxide: Heme *d* binds CO with high affinity. *Biochemistry (Moscow)*. 2008; 73:14–22. (translated from *Biokhimiya* (in Russian) (2008), 73, 18–28). [PubMed: 18294124]
57. Muntyan MS, Bloch DA, Drachev LA, Skulachev VP. Kinetics of CO binding to putative Na<sup>+</sup>-motive oxidases of the *o*-type from *Bacillus FTU* and of the *d*-type from *Escherichia coli*. *FEBS Lett.* 1993; 327:347–350. [PubMed: 8348962]
58. Junemann S, Wrigglesworth JM, Rich PR. Effects of *decyl*-aurachin D and reversed electron transfer in cytochrome *bd*. *Biochemistry*. 1997; 36:9323–9331. [PubMed: 9235974]
59. Lorence RM, Miller MJ, Borochoy A, Faiman-Weinberg R, Gennis RB. Effects of pH and detergent on the kinetic and electrochemical properties of the purified cytochrome *d* terminal oxidase complex of *Escherichia coli*. *Biochim. Biophys. Acta.* 1984; 790:148–153. [PubMed: 6386051]



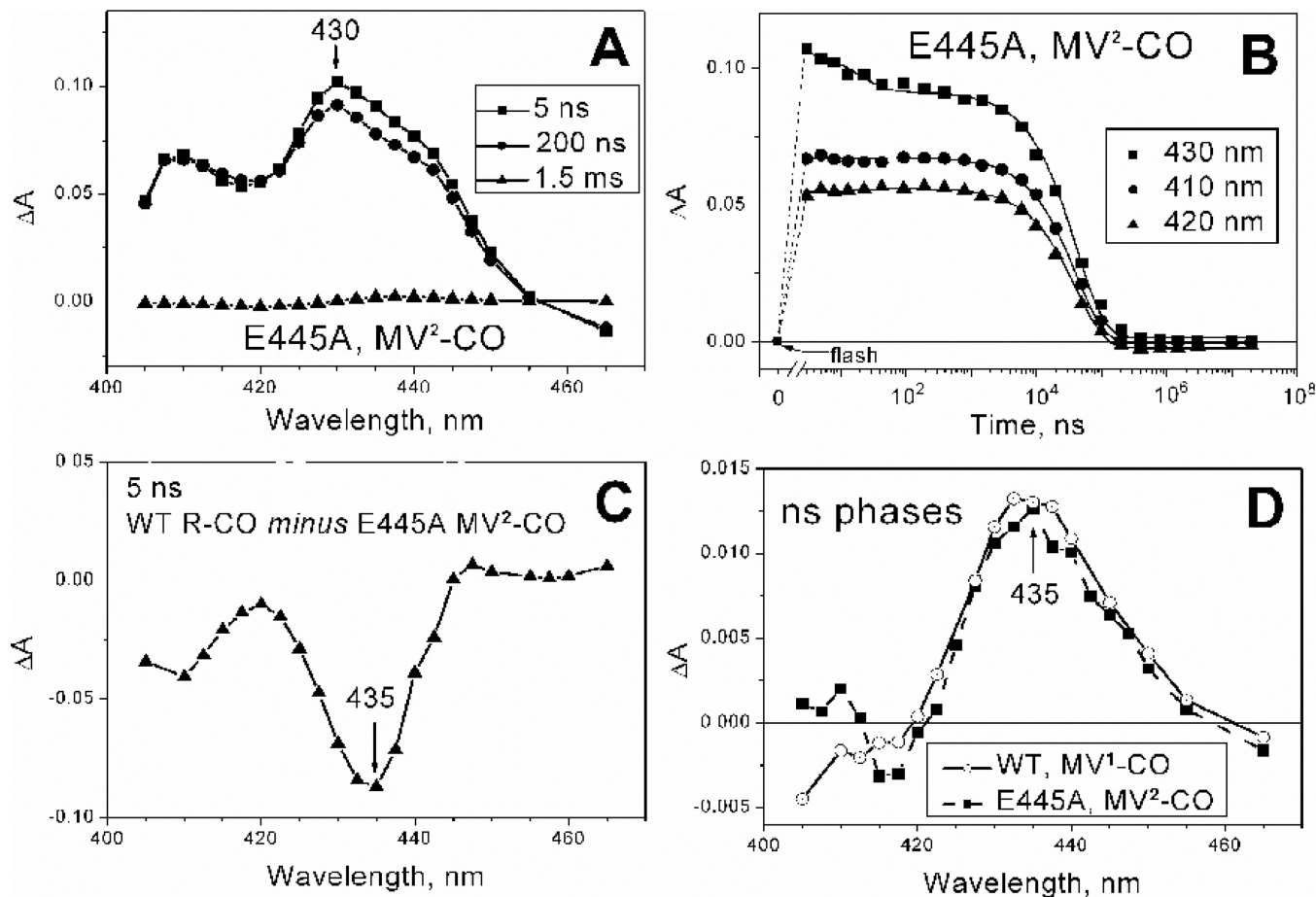


**Fig. 1.**

Absorption changes measured after photodissociation of CO from the *E. coli* membranes containing the WT cytochrome *bd* in the R-CO state. *Main panel:* Kinetics of absorption changes at selected wavelengths during CO recombination. The kinetic data points (symbols) are shown with their best fits to single exponentials (solid lines) yielding  $\tau \sim 12 \mu\text{s}$ . Arrow indicates the moment of laser flash. *Inset:* Transient absorption spectrum at a delay time of 5 ns. For conditions, see the Materials and methods section.

**Fig. 2.**

Absorption changes measured after photodissociation of CO from the *E. coli* membranes containing the WT cytochrome *bd* in the MV<sup>1</sup>-CO state. (A) Transient absorption spectra at delay times of 5 ns, 200 ns, and 60  $\mu$ s. (B) Kinetics of absorption changes at selected wavelengths during CO recombination. The kinetic data points (symbols) are shown with their best fits (solid lines). The kinetics at 435 nm is fitted to the sum of three exponentials yielding  $\tau \sim 14$  ns, 14  $\mu$ s, and 280  $\mu$ s. 417.5 nm has been selected as the wavelength isosbestic for the 14 ns and 280  $\mu$ s components, therefore for that kinetics a one-exponential fit with  $\tau \sim 14$   $\mu$ s is sufficient. Arrow indicates the moment of laser flash. (C) Spectra of the absorption changes associated with the 14-ns, 14- $\mu$ s, and 280- $\mu$ s components. The spectrum of the 14-ns phase is calculated as the difference between the transient spectra measured at delay times of 5 ns and 200 ns. The spectrum of the 280- $\mu$ s phase is the spectrum measured 60  $\mu$ s after the flash. The amplitude of the latter has been divided by  $e^{-60/280}$  to correct for the decay at 60  $\mu$ s. The spectrum of the 14- $\mu$ s phase is calculated as the difference between the transient spectrum measured at a delay time of 200 ns and the spectrum of the 280- $\mu$ s phase. (D) Difference between R-CO and MV<sup>1</sup>-CO transient spectra at a delay time of 5 ns. The spectra are normalized at 445 nm (spectrum MV<sup>1</sup>-CO multiplied by 7.5) as the spectral properties at this wavelength are independent of the oxidation state of the *b*-hemes [41].

**Fig. 3.**

Absorption changes measured after photodissociation of CO from the *E. coli* membranes containing the E445A mutant cytochrome *bd* in the MV<sup>2</sup>-CO state. **(A)** Transient absorption spectra at delay times of 5 ns, 200 ns, and 1.5 ms. **(B)** Kinetics of absorption changes at selected wavelengths during CO recombination. The kinetic data points (symbols) are shown with their reasonable fits to the sum of two exponentials (solid lines) yielding  $\tau \sim 14$  ns, and 42  $\mu$ s. Approximation with three exponentials does not improve the fit significantly. Arrow indicates the moment of laser flash. **(C)** Difference between transient absorption spectra of the WT cytochrome *bd* in the R-CO state and the E445A mutant cytochrome *bd* in the MV<sup>2</sup>-CO state at a delay time of 5 ns (normalized at 445 nm). **(D)** Comparison of the spectra of the absorption changes associated with the nanosecond components for the WT cytochrome *bd* in the MV<sup>1</sup>-CO state and the E445A mutant cytochrome *bd* in the MV<sup>2</sup>-CO state (normalized on the maximum). The latter spectrum is a difference between the MV<sup>2</sup>-CO E445A transient spectra at delay times of 5 ns and 200 ns.

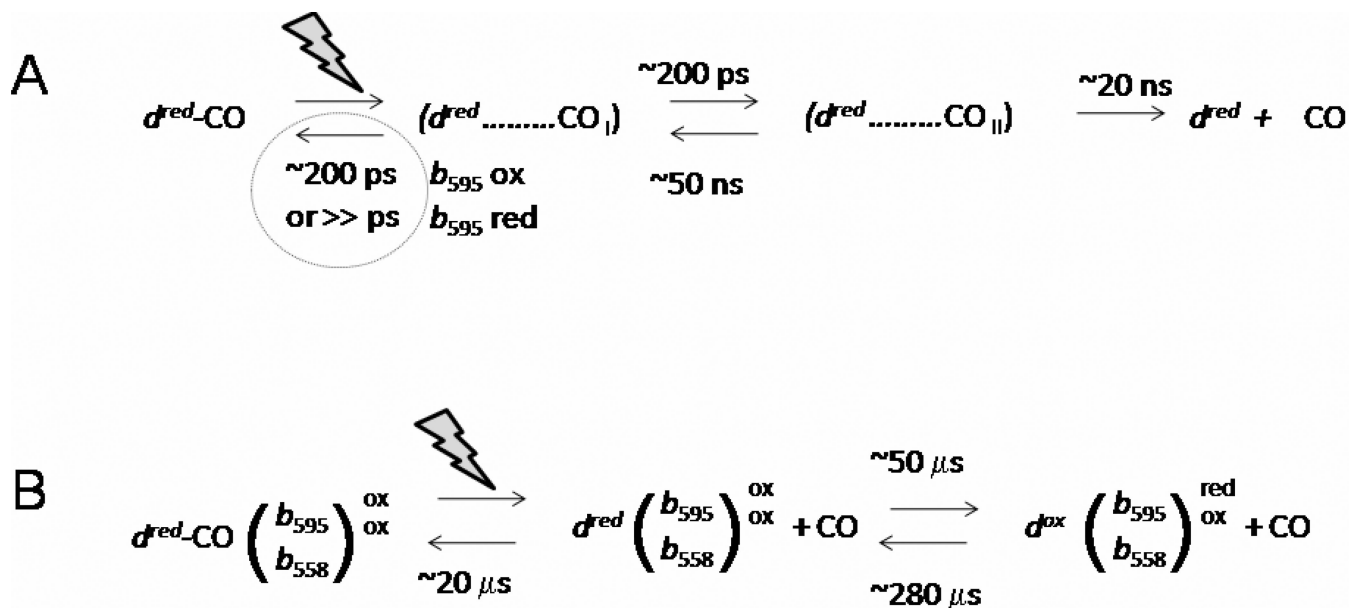


Fig. 4.

(A) Minimal scheme of geminate recombination phases of CO starting from the MV<sup>1</sup>-CO and R-CO states. Two different configurations of dissociated CO in the protein ( $d^{\text{red}} \dots \text{CO}_i$ ;  $i=I, II$ ) are required to explain the two geminate recombination phases. The ratio of forward and backward rates from these configurations is roughly estimated from the amplitudes of the phases; the sums of the rates correspond to the experimentally observed rates. The state ( $d_{\text{red}} + \text{CO}$ ) denotes a state where CO has escaped from the protein. In this minimal scheme, if heme  $b_{595}$  is reduced prior to dissociation of the heme  $d$ -CO bond, geminate recombination from the ( $d_{\text{red}} \dots \text{CO}_I$ ) state does not compete efficiently with population of the ( $d^{\text{red}} \dots \text{CO}_{II}$ ) state. (B) Minimal scheme of bimolecular CO recombination and electron transfer starting from the MV<sup>1</sup>-CO. The first dissociation step comprises all steps in scheme (A). The ratio of forward and backward rates from the CO dissociated  $d_{\text{red}}$  is roughly estimated from the amplitudes of the phases; the sums of the rates correspond to the experimentally observed rates.